The rice OsRad21-4, an orthologue of yeast Rec8 protein, is required for efficient meiosis

Liangran Zhang[1,2], Jiayi Tao[1,2], Shunxin Wang[1], Kang Chong[1] and Tai Wang[1,*]

[1]*Key Laboratory of Photosynthesis and Environmental Molecular Physiology, Research Center of Molecular & Developmental Biology, Institute of Botany, Chinese Academy of Sciences, Beijing 100093, China;* [2]*Graduate School of the Chinese Academy of Sciences, Beijing 100049, China (*author for correspondence; e-mail twang@ibcas.ac.cn)*

Abstract

In yeast, Rad21/Scc1 and its meiotic variant Rec8 are key players in the establishment and subsequent dissolution of sister chromatid cohesion for mitosis and meiosis, respectively, which are essential for chromosome segregation. Unlike yeast, our identification revealed that the rice genome has 4 *RAD21*-like genes that share lower than 21% identity at polypeptide levels, and each is present as a single copy in this genome. Here we describe our analysis of the function of *OsRAD21-4* by RNAi. Western blot analyses indicated that the protein was most abundant in young flowers and less in leaves and buds but absent in roots. In flowers, the expression was further defined to premeiotic pollen mother cells (PMCs) and meiotic PMCs of anthers. Meiotic chromosome behaviors were monitored from male meiocytes of OsRAD21-4-deficient lines mediated by RNAi. The male meiocytes showed multiple aberrant events at meiotic prophase I, including over-condensation of chromosomes, precocious segregation of homologues and chromosome fragmentation. Fluorescence *in situ* hybridization experiments revealed that the deficient lines were defective in homologous pairing and cohesion at sister chromatid arms. These defects resulted in unequal chromosome segregation and aberrant spore generation. These observations suggest that OsRad21-4 is essential for efficient meiosis.

Introduction

Sister chromatid cohesion is essential for accurate chromosome segregation during mitosis and meiosis. In *Saccharomyces cerevisiae* and *Schizosaccharomuces pombe*, the cohesion is established in the S phase to link newly replicated sister chromatids until the metaphase–anaphase transition and is mediated by a phylogenetically conserved multiprotein complex called cohesin (Guacci *et al.*, 1997; Michaelis *et al.*, 1997; Uhlmann and Nasmyth, 1998). Mitotic cohesin in both fission and budding yeast involves at least Rad21/ Scc1, Scc3,

Smc1 and Smc3 (Birkenbihl and Subramani, 1992; Guacci *et al.*, 1997; Michaelis *et al.*, 1997; Tomonaga *et al.*, 2000). The mitotic cohesion between sister chromatids occurs by a proteinaceous ring, in which Rad21/Scc1, via its conservative N- and C-terminal domains, bridges heads of the heterodimer of Smc1–Smc3 (the structural maintenance of chromosomes) (Nasymth, 2002; Gruber *et al.*, 2003). At the metaphase–anaphase transition, proteolytic cleavage of Rad21/Scc1 mediated by separase triggers dissociation of cohesion proteins from chromosomes. The cleavage is necessary and sufficient for sister separation (Uhlmann

et al., 2000; Tomonaga *et al.*, 2000; Lee and Orr-Weaver, 2001; Nasmyth, 2001).

Meiosis is a specialized cell cycle in which a single round of DNA replication is followed by two rounds of successive chromosome segregation. This cycle adopts a mechanism different from that of mitosis to ensure faithful disjunction of homologous chromosomes at meiosis I, where meiocytes dissolve cohesion along sister arms but retain the cohesion at sister centromeres. The centromeric cohesion persists until the onset of anaphase II, and then its release leads to segregation of sister chromatids. Therefore, in meiotic cohesion of both fission and budding yeast, Rad21 is replaced by its meiotic variant Rec8 (Klein *et al.*, 1999; Wanatabe and Nurse, 1999), and the other three subunits are common to mitotic counterparts. The mutation in the *REC8* locus of yeast disrupts cohesion at both sister arms and centromeres, leading to precocious segregation of sister chromatids at meiosis I. Thus, Rec8 has specificity for differential release of the chromosome arm and centromeric cohesion in meiosis I and II (Buonomo *et al.*, 2000; Nasmyth, 2001; Kitajima *et al.*, 2003a, b) This protein is also required for homologue pairing in yeast (Klein *et al.*, 1999).

In recent years, homologs of yeast Rec8 have been identified in *Caenorhabditis elegans* (CeRec8) (Pasierbek *et al.*, 2001), mice (MmRec8), humans (HsRec8) (Parisi *et al.*, 1999) and Arabidopsis (Syn1) (Bai *et al.*, 1999; Bhatt *et al.*, 1999; Cai *et al.*, 2003). Further genetic analysis of CeRec8 and Syn1 has revealed that the primary function of Rec8 in regulating sister chromatid cohesion and homologous chromosome (homologue) pairing was conserved in *Caenorhabditis elegans* and Arabidopsis. However, the two higher eukaryotic mutants showed clear phenotypic differences with yeast *rec8* mutants. In *C. elegans*, RNAi-mediated Rec8 deficiency led to abnormal pairing of homologues and the cohesion defect both at sister arms and at centromeres in meiosis I, a similar phenotype occurring in the yeast rec8 mutants. The protein deficiency in the worm also caused chromosome fragmentation (Pasierbek *et al.*, 2001). In Arabidopsis, a mutation in *SYN1* locus disrupted homologous pairing and sister-arm cohesion, but seems not to affect centromeric cohesion. In addition, this mutant showed chromosome fragmentation and abnormal chromosome condensation (Bai *et al.*, 1999; Cai *et al.*, 2003). The

phenotypic difference between yeast and higher eukaryotes suggests an evolution in the mechanism underlying meiosis in higher organisms because they must handle an enlarged genome size (in number and length of chromosomes) and increased proportion of repetitive sequences to ensure faithful segregation of chromosomes.

Indeed, in fission yeast, which shares a heterochromatin-containing centromeric structure with higher eukaryotes (Kitajima *et al.*, 2003a, b), the function of Rec8 in establishing sister arm and centromere cohesion is regulated by its partners Psc3, the ubiquitous version of Scc3, and Rec11, a meiosis-specific variant of Scc3, respectively (Kitajima *et al.*, 2003a, b). And Rec11 is absent in budding yeast (Watanabe, 2004). Mammalian meiotic cells have SMC1β and STAG3, each representing the meiotic variant of Smc1 and Scc3 (Prieto *et al.*, 2001; Revenkova *et al.*, 2001; Petronczki *et al.*, 2003), and STAG3 might play a role similar to that of Rec11 (Watanabe, 2004). Interestingly, unlike yeast and vertebrates that have 2 Rad21 proteins (Rad21 and its meiotic variant Rec8), the Arabidopsis genome contains at least 3 *RAD21*-like genes (Bai *et al.*, 1999; Dong *et al.*, 2001; Cai *et al.*, 2003), and *C. elegans* has 4 *RAD21*-like genes (Pasierbek *et al.*, 2001; Mito *et al.*, 2003). However, in higher organisms, the roles of Rec8 proteins in meiosis have been characterized to date by mutation only from *C. elegans* and Arabidopsis, whereas *C. elegans* seems to have a mechanism for meiotic prophase I different from that of other higher organisms (Grelon *et al.*, 2001; Kitajima *et al.*, 2003a, b) in some aspects. Remarkably, in plants and yeast, recombination and synapsis is tightly coupled (Grelon *et al.*, 2001; Kitajima *et al.*, 2003a, b; Li *et al.*, 2005), while in this worm, pairing and synapsis can occur independently of recombination (Dernburg *et al.*, 1998). So, we still remain ignorant about the molecular regulation of meiosis, specifically of prophase I, of higher organisms. To understand the mechanism promoting cohesion and its coordination relation with other early events of prophase I, further studies involving other model organisms are necessary.

Besides Arabidopsis, rice represents another excellent system for studying the molecular mechanism of meiosis because (1) its genome is mid-sized, with 12 pairs of chromosomes, and has been sequenced; (2) an efficient transgenic system

established in rice can be used to dissect genetic function by reverse genetics; and (3) meiosis in rice differs from that of Arabidopsis in some cytological characteristics, such as rice meiosis I is followed by the formation of a cell plate, instead of a organelle band reported in Arabidopsis, between the two daughter cells (Chen *et al.*, 2005). Therefore, we identified *RAD21*-like genes from rice and found 4 *RAD21*-like genes (Zhang *et al.*, 2004 and this study). Furthermore we characterized *OsRAD21-4*, whose protein formed a clade with Arabidopsis Syn1 in a phylogenetic analysis. Its mRNA and protein were expressed preferentially in young flowers where the pollen mother cells (PMCs) were in pre-meiotic stages. Furthermore, knock-down experiments by RNA interference (RNAi) indicated that the gene was essential to meiosis. OsRAD21-4-deficient plants mediated by RNAi showed multiple aberrant events at meiotic prophase I, including over-condensation of chromosomes, precocious segregation of homologues and chromosome fragmentation. Fluorescence *in situ* hybridization experiments revealed that the deficient lines were defective in homologous pairing and cohesion at sister chromatid arms. These defects resulted in unequal chromosome segregation at anaphase I, and, finally, abnormal spores. This study is the first insight into the molecular regulation of meiotic cohesion in monocots and provides useful information to understand the relation of cohesion to other early events of meiosis prophase I.

Materials and methods

Plant materials

Cultivar Zhonghua 10 (*Oryza sativa* L. ssp. *japonica*) was grown under standard conditions. Flowers in which PMCs were in pre-meiotic, meiotic, and uninucleate microspore stages were collected. Leaves were collected from 3-week-old plants. Roots (about 2 mm in length) and buds were harvested from seedlings germinated on sterile-water-soaked papers.

Extraction of nucleic acids

Total RNA was isolated with use of a Trizol kit (Invitrogen) according to the manufacturer's protocol,

and treated with RNase-free DNase I (TaKaRa) to remove residual genomic DNA. Genomic DNA was extracted from seedlings by use of cetyltrimethylammonium bromide (CTAB) according to the method of Murray and Thompson (1980).

OsRAD21-4 cDNA cloning

An open reading frame (ORF) encoding a proposed Rad21-like polypeptide was predicted by a tblastn search of the TIGR database with use of the OsRad21-1 amino acid sequence (Zhang *et al.*, 2004) as a query. The Rad21-like protein had N and C domains conserved in Rad21/Rec8 proteins. In our lab, the protein was named OsRad21-4. The cDNA sequence of OsRad21-4 ORF was obtained by RT-PCR with use of the first-strand cDNA synthesized from flower RNA as a template and the primer pair P1 (5′-ATGGCACTAAGGCTCTCC-3′) and P2 (5′-ATAGAAGAGTCGGGCAGC-3′), designed according to the searched genomic sequence. Furthermore, 3′ and 5′ RACE were performed to obtain 3′ and 5′ terminal sequences, respectively, of the cDNA by the method of Ding *et al.* (2002). The gene-specific primers for 3′ RACE were P3 (5′-GAAGTACAGTTGCCATCC-3′) and P4 (5′-AGGCTTTCAGATGTTGGG-3′), and for 5′ RACE, P5 (5′-ATCCAAATCCTCCAAACG-3′) and P6 (5′-TCATACTTGGCTTGGGTT-3′). RT-PCR was used to confirm mRNA with use of the primer pair P7 (5′-CTCACTCGCTCATCCATT-3′) and P8 (5′-CATCTTTGGTCCCCTTGA-3′).

The amplified cDNA fragments were gel-purified, cloned into the pGEM-T vector (Promega) and confirmed by sequencing.

Southern blot hybridization

Twenty micrograms of genomic DNA was digested with *Eco*RV, which cuts once in the RNAi construct pRAD21-4i outside the transgene-coding region (see RNAi Interference Construction and Plant Transformation). After the digested DNA was subjected to electrophoresis on a 0.8% agarose gel, the DNA fragments were blotted onto a Hybond N+ nylon membrane (Amersham). Hybridization was carried out with a ^{32}P-labeled DNA fragment of the hygromycin gene at 42 °C overnight. The filter was washed with 2×SSC and 0.5% SDS for 20 min at 37 °C, and then with

0.1×SSC and 0.5% SDS for 20 min at 65 °C. The resulting filter was autographed at −80 °C.

Semi-quantitative RT-PCR and in situ hybridization

Semi-quantitative RT-PCR was conducted with the primers P9 (5′-CAG AAT TCG GAA TGC GTT TGG AGG AT-3′) and P10 (5′-CAG AAT TCG GAA TGC GTT TGG AGG AT-3′) to analyze mRNA accumulation in organs. The amplified tubulin tubA cDNA (accession no. X91806) was used as a control (Ding et al., 2002). First-strand cDNA was synthesized with SuperScript II RNase H⁻ reverse transcriptase (200 U/µl, GIBCO-BRL) according to the manufacturer's protocol. PCR was performed in a mixture of 50 µl that contained 1 µl of first-strand cDNA, 10 pmol each of the gene-specific primers, 0.4 mM dNTPs, 1× PCR buffer and 2.5 U LATaq DNA polymerase (5 U/µl, TaKaRa) for 25 cycles.

For in situ hybridization, DIG-labeled sense and antisense RNA probes were synthesized with T7 or SP6 RNA polymerase (Roche) from a linearized plasmid containing a 3′ cDNA fragment of this gene. Other procedures were followed the methods of Ding et al. (2002).

Preparation of the polyclonal antibody against OsRad21-4

To generate an antibody to OsRad21-4, a partial cDNA sequence encoding the polypeptide fragment spanning amino acids 138 to 387 of OsRad21-4 was amplified by PCR with primers P9/P10. After being confirmed by sequencing, the amplified cDNA fragment was digested with EcoRI and SalI and ligased in-frame into the glutathione S-transferase (GST) gene fusion vector pGEX-4T-3 (Amersham), generating the plasmid pGE21-4. Furthermore, E. coli strain DH5, harboring pGE21-4, was cultured in LB medium at 37 °C. After reaching an exponential phase, the culture was induced immediately with 2 mM isopropyl-b-D-thiogalactoside (IPTG) and then incubated for 2 h at 37 °C with vigorous shaking. Cells were collected by centrifugation, lysed with lysozyme according to the method of Worrall (1996), and then the recombinant protein was purified by affinity chromatography with use of glutathione sepharose 4B of the GST Purification Modules (Amersham).

The purified recombinant protein was used to inject rabbits to generate polyclonal antibody according to the standard protocol (Hanly et al., 1995).

Western blot analysis

Total proteins from different organs were extracted according to the method of Salekdeh et al. (2002) and dissolved in SDS sample buffer (Laemmli, 1970). SDS-PAGE was performed with use of 4.5% stocking and 12% separating acrylamide gels (Laemmli, 1970). A low-molecular-mass protein marker kit (14–97 kDa, Sangon) was used to determine approximate protein sizes. Proteins in gels were visualized on 0.1% Coomassie brilliant blue R-250 staining in 50% ethanol and 10% acetic acid.

For western blot analysis, proteins in gels were electrophoretically transferred on a semidry blot apparatus to a polyvinylidene difluoride (PVDF) membrane (Pierce) with a buffer of 10 mM 3-cyclohexylamino-1-propanesulfonic acid (CAPS) and 10% (v/v) methanol at 2 mA constant current per cm² gel for 1 h. After being blocked with a blocking buffer [3% BSA in TBS buffer (20 mM Tris–Cl, pH 7.5, 150 mM NaCl)] and washed with TTBS (0.05% Tween-20, 20 mM Tris–Cl, pH 7.5, 150 mM NaCl), the membrane was incubated with a polyclonal antibody to OsRad21-4 (1:10000 dilution) or tubulin (1:5000 dilution, Sigma) in the blocking buffer for 1 h, washed with TTBS and TBS buffer, and then incubated for 1 h with goat anti-rabbit IgG-conjugated alkaline phosphatase (1:2000 dilution, Sino-Amico Corp). After hybridized membranes were washed, positive signals were visualized with use of 0.1 mg ml⁻¹ 5-bromo-4-chloro-3-indolyl phosphate and 0.2 mg ml⁻¹ nitroblue tetrazolium (Sigma) in a buffer of 100 mM Tris–HCl pH 9.5, 100 mM NaCl and 5 mM MgCl₂.

Subcellular localization

The cDNA fragment spanning the whole ORF of OsRAD21-4 was amplified with use of the primers P11 (5′-CGCAGATCTCTCACTC GCTCATCC-ATT-3′, with an added BglII site underlined) and P12 (5′-GCTCTAGACATCTTTGTCCCCTTG A-3′, with an added XbaI site underlined), digested with both BglII and XbaI and then inserted into the BgII/SpeI-linearized pCAMBIA1302 vector

(CAMBIA) (SpeI and XbaI are isocaudiners). The resulting construct pOsRAD21-4::GFP, which contains the fusion of OsRAD21-4::GFP under a CaMV35S promoter, was confirmed by sequencing and transformed into onion epidermis mediated by *Agrobacterium tumefaciens* according to the method of Yang *et al.* (2000). GFP fluorescence signals were detected under a microscope with a FITC filter (Zeiss).

RNA interference construction and plant transformation

To obtain a vector for RNAi construction, a fragment spanning CaMV 35S::GusA:Tnos from pBI121 (Clontech) was cut with *Eco*RI/*Hin*dIII and inserted into *Eco*RI/HindIII-linearized pCAMBIA1300 (CAMBIA) to generate an immediate vector. Furthermore, the sequence of GusA in the immediate vector was replaced with a 640-bp XbaI-SacI spacer sequence flanked by 2 35-bp sequences, 1 of which contained 6 multiple cloning sites and another 5 sites, to finally generate an RNAi vector termed pWTC605 (Figure 5A), which was confirmed by sequencing.

For the RNAi construct, the first cDNA segment spanning the middle region (nt 468-1236) of OsRAD21-4 cDNA, with no shared similarity to cDNA sequences of 3 other RAD21-like genes identified in the rice genome, was amplified by PCR with use of the primer pair P13 (5′-AG<u>TCTAGA</u>GGGAATGCGTTTGGA GAT-3′, *Xba*I site is underlined) and P14 (5′-TA <u>GGTACC</u>TGGGTTGGAAATGCCTGA-3′, *Kpn*I site is underlined). The second fragment was amplified with use of primer pair P15 (5′-TA <u>GAGCTC</u>GGGATGCGTTTGGAGGAT-3′, *Sac*I site is underlined) and P16 (5′-TA<u>GTGAC</u>TG GGTTGGAAATGCCTGA-3′, *Sal*I site is underlined), which was identical to the first one except for the recognition sites of restriction enzymes embedded in the primers used. The design resulted in insertion of the 2 cDNA fragments into pWTC605 in the sense and antisense orientations, intervened by the spacer (Figure 5A). The resulting RNAi construct, pRAD21-4i, was first introduced into *A. tumefaciens* strain EHA105 and then into rice embryonic calli to generate RNAi plants according to the method described by Hiei *et al.* (1994).

Small RNA isolation and detection

Isolation and visualization of OsRAD21-4 specific small RNA in transgenic RNAi rice followed the method of Hamilton and Baulcombe (1999) with some modifications. Briefly, total RNA was isolated with Trizol (Invitrogen) according to the manufacturer's protocol. After removal of high-molecular-weight RNA by precipitation with 5% polyethylene glycol 8000 and 0.5 M NaCl, low-molecular-weight RNA was re-precipitated from the resulting supernatant with 3 volumes of ethanol and a 1/10 volume of NaAc (3 M, pH 5.2), separated by electrophoresis on 8% polyacrylamide-7 M urea−0.5× Tris–borate EDTA gels, and finally transferred electrophoretically onto Hybond N+ nylon membrane (Amersham) on a semidry blot apparatus. The membrane was pre-hybridized with a buffer of 0.125 M Na_2HPO_4–NaH_2PO_4 (pH 7.2) containing 7% SDS and 0.25 M NaCl at 47 °C and hybridized in the same solution containing the OsRAD21-4 cDNA probe labeled with $\alpha-^{32}P$-dCTP by use of the Prime-a-gene kit (Promega). The resulting membrane was autographed at −80 °C.

Meiotic chromosome spreads

Meiosis chromosome spreads and 4′,6-Diamidino-2-phenylindole (DAPI) staining were performed according to Ross *et al.* (1996) with some modifications. Flowers fixed in Carnoy's solution were washed with 10 mM citrate buffer (pH 4.5) and digested with 0.3% cellulase (Yakult Corp) and 0.3% pectolyase (Yakult Corp) in the citrate buffer at 37 °C for 30 min. After being washed with the same buffer, the digested anthers were placed in a small drop of 60% acetic acid on a slide and squashed with a cover slip to release PMCs. Before observation under a fluorescent microscope (ZEISS AXIOSKOP40 with HBO100), 5 μl of DAPI antifade solution [1 μg/ml DAPI, 50% glycerol, 10 mM citrate buffer (pH 4.5), and 25 μg/ml DABCO (1,4-diazabicyclo[2.2.2]octane)] was added onto the slide, which was then covered with a glass cover and sealed with nail polish.

Fluorescence in situ *hybridization (FISH)*

The chromosome slides were prepared as described in "Meiotic chromosome spreads". The 25S

rDNA (Takaiwa *et al.*, 1985) probe was labeled by PCR using the primer pair 5′-CTGTGAAGGGT TCGAGTTGG-3′ and 5′-TTGCTACTACCAAG ATCTG-3′ and a dNTP mixture containing digoxigenin-labeled dUTP (Roche). The centromere probe CentO (Cheng *et al.*, 2002) was labeled with digoxigenin-labeled dUTP by a random primer method (Promega). FISH was performed according to the method of Jiang *et al.* (1995) and the probed sites were detected by rhodamin-conjugated anti-digoxigenin antibody (Roche). Moreover, these chromosomes were counter-stained with 1 μg/ml DAPI. Chromosomes stained with FISH and DAPI were observed under a fluorescence microscopy (Zeiss). Images obtained by cool CCD were adjusted and merged with Image-Pro Plus (IPP) 5.0 software.

Computer analysis

We performed a BLAST search of the TIGR rice genomic database for the genomic sequence of this gene. Potential nuclear localization signals were identified by use of PredictNLS (http://cubic.bioc.columbia.edu/). The potential recognition sites of separase were predicted according to this motif (XXS/E/DXEXXRXXX). The PEST motif was identified by use of the PESTfind program (http://emb1.bcc.univie.ac.at/embnet/tools). Other motifs were searched by use of SMART (http://smart.embl-heidelberg.de/) and Motif scan (http://myhits.isb-sib.ch/cgi-bin/motif_scan). The degree of amino acid sequence similarity was determined by use of the BLAST program. Multiple sequence alignments involved use of Clustal W (v.1.81 in DDBJ).

DNA sequence analysis

DNA was sequenced by the dideoxy chain termination method with use of an automated sequencer model 377 (Applied Biosystems).

Results

Cloning of OsRAD21-4 cDNA

Our TBLASTN search of rice genomic sequences in TIGR, using the OsRad21-1 amino acid sequence (accession no. AY288943, Zhang *et al.*, 2004) as a query, enabled us to predict 3 other open reading frames (ORFs) encoding probable Rad21-like proteins in the rice genome, each of which contains the N-terminal domain Pfam04825 and the C-terminal domain Pfam04824, which are conserved in known Rad21/Rec8 proteins from different species (Zhang *et al.*, 2004). Their cDNAs were cloned (data not shown) and deposited in the GenBank database (accession No. AY371047, AY371048 and AY371049). The genes corresponding to each cDNA was named *OsRAD21-2* (localized in chromosome 4), *OsRAD21-3* (in chromosome 8) and *OsRAD21-4* (in chromosome 5) in our lab. OsRAD21-4 cDNA cloned here (see Materials and methods) is 2133 bp long and has a 5′ UTR of 54 bp, a 3′ UTR of 255 bp and an ORF of 1824 bp encoding a deduced polypeptide of 608 amino acids (OsRad21-4). OsRad21-4 has a calculated molecular mass of 68.5 kDa and an isoelectric point (pI) of 5.45.

The genomic sequence of *OsRAD21-4* was further confirmed by BLASTN searches of the TIGR rice genomic database with use of its full-length cDNA sequence as a query. This cDNA had a hit only from the long arm of chromosome 5 (AC120988 or AC007858) with 100% identity over the cDNA sequence, which suggests that the gene is present in the rice genome as a single-copy gene. Comparison of this cDNA to its genomic DNA sequence revealed that a 7.5-kb genomic DNA sequence spanning all exons represents *OsRAD21-4*. It is composed of 20 exons and 19 introns (Figure 1), which were spliced out by canonical GT-AG sites. Pairwise comparison did not detected obvious sequence similarity between Os-RAD21-4 cDNA and any cDNA of the other three rice Rad21 homologs (data not shown).

OsRad21-4 is close to Rec8 proteins of the Rad21/Rec8 family

OsRad21-4 is a relatively hydrophilic protein and contains the entire Pfam04825 and Pfam04824 domains (spanning amino acids 1–115 and 554–608, respectively) (Figure 2A), of which Pfam04825 is highly conserved in all known members and Pfam04824 present in most of the Rad21/Rec8 family (Zhang *et al.*, 2004). The two domain regions are spaced by a long linker sequence (amino acids 116-553), which showed no similarity to other members of this family. This
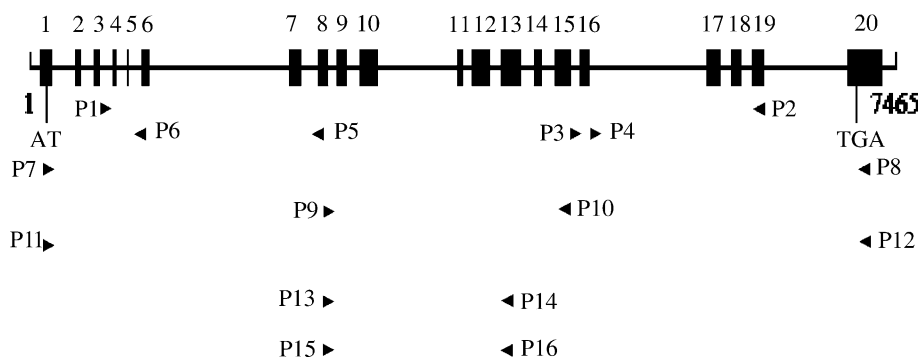
Figure 1. Schematic organization of a 7.5-kb genomic fragment of chromosome 5 carrying *OsRad21-4*. The exons were determined by comparing the DNA sequence with its cDNA sequence and shown as black boxes. The position and direction of primers used in this study are shown as arrows below the map.

linker sequence contains a potential nuclear targeting motif at positions 272–279 (KRKKRRKD), 2 separase recognition sites at 411–421 (ADDIEKLRGNT) and 420–430 (NTSGEYGRDYD) and a PEST motif at 511–534 (RLSDVGPTPDLLEEIEPTQTPYEK) (Figure 2A). These motifs are also present in other known Rad21/Rec8 proteins (Zhang et al., 2004) and are proposed to be implicated in function regulation in cohesion establishment and disassociation (Nasmyth, 2001).

OsRad21-4 only displayed a limited similarity with the other three rice Rad21 homologs (23% amino acid identity to OsRad21-1, 16% to OsRad21-2 and 20% to OsRad21-3). The similarities mainly occurred in their N- and C-domain regions along with no similarity between their middle linker regions. Furthermore, multiple alignments of OsRad21-4 with other known Rad21/Rec8 sequences revealed that OsRad21-4 was more similar to Arabidopsis Syn1 (41% amino acid identity) than to the others (less than 21% identity). Because the N-terminal Pfam04825 domain is highly conserved in all the known Rad21/Rec8 proteins but not C-terminal Pfam04824 (Zhang et al., 2004), we performed a phylogenetic analysis involving Clustal W alignments of Pfam04825-containing N-terminal sequences of these proteins. As shown in Figure 2C, OsRad21-4 tended to group with the known Rec8 proteins from fission, mice, humans and Arabidopsis (Parisi et al., 1999; Watanabe and Nurse, 1999; Bai et al., 1999; Pasierbek et al., 2001; Lee et al., 2003), and formed a clade with Syn1. These data suggest that OsRad21-4 is a rice orthologue of yeast Rec8.

The features of relative hydrophilicity, acidic pI and nuclear targeting signal-containing motifs, described in OsRad21-4 above, indicate that this protein has a potential nucleus-localizing function; therefore, we used transient transformation to investigate its subcellular localization. Compared with uniform GFP signals detected in control cells transformed with pCAMBIA1302, the GFP signals of the OsRad21-4::GFP fusion were localized mostly in nuclei (Figure 2B) with weak signals detected in cytoplasm, which indicates that this protein is a nucleus-localizing protein.

OsRad21-4 is expressed preferentially in premeiotic PMCs

To obtain information about the function of this gene, we used semi-quantitative RT-PCR to analyze its expression in buds, roots, leaves and flowers where PMCs were in the meiotic phase. As shown in Figure 3A, this gene was expressed preferentially in flowers, weakly in leaves and barely in buds and roots. Furthermore, immunoblot analysis with the antibody to OsRad21-4 revealed that the protein was most abundant in flowers, hardly detectable in leaves and buds, and undetectable in roots, which demonstrates that OsRad21-4 mRNA and protein were mainly confined to flowers (Figure 3B).

Moreover, to understand the accumulation patterns of OsRad21-4 transcript in developing flowers, we first collected flowers in different developmental stages based on the length of flowers in combination with cytological observations. Flowers of 0.9 mm in length were pooled as F1, 0.9–2.5 mm as F2, 2.5–5.0 mm as F3 and

(A) <u>MFYSHQLLARKAPLGQIWMAATLHSKINRKRLDKLDIIKICEEILNPSVPMALRLSGILMGG</u>
<u>VAIVYERKVKALYDDVSRFLIEINEAWRVKPVADPTVLPKGKTQAKYEAVTLP</u>ENIMDMDVE
QPMLFSEADTTRFRGMRLEDLDDQYINVNLDDDDFSRAENHHQADAENITLADNFGSGLGET
DVFNRFERFDITDDDATFNVTPDGHPQVPSNLVPSPPRQEDSPQQQENHHAASSPLHEEAQQ
GGASVKNEQEQQKMKGQQPAKSS**KRKKRRKD**DEVMMDNDQIMIPGNVYQTWLKDPSSLITKR
HRINSKVNLIRSIKIRDLMDLPLVSLISSLEKSPLEFYYPKELMQLWKECTEVKSPKAPSSG
GQQSSSPEQQQRNLPPQAFPTQPQVDNDREMGFHPVDF*ADDIEKLRGNT SGEYGRDYD*AFH
SDHSVTPGSPGLSRRSASSSGGSGRGFTQLDPEVQLPSGRSKRQHSSGKSFGNLDPVEEEFP
FEQELRDFKMRRLSDVGPTPDLLEEIEPTQTPYEKKSNPIDQVTQSIHSYLKLHFDTP<u>GASQ</u>
<u>SESLSQLAHGMTTAKAARLFYQACVLATHDFIKVNQLEPYGDILISRGPKM</u>

(B)

(C)
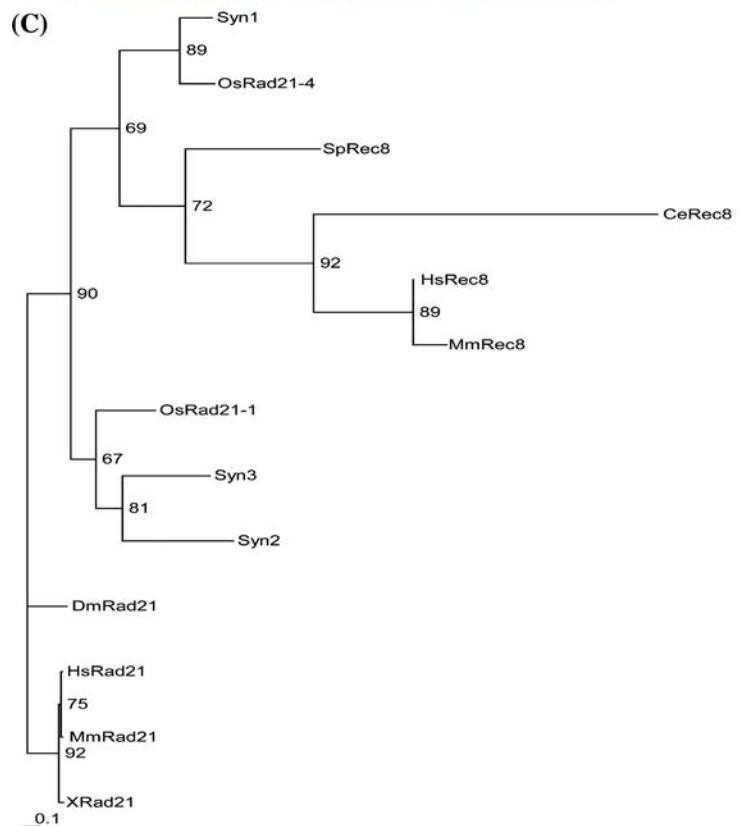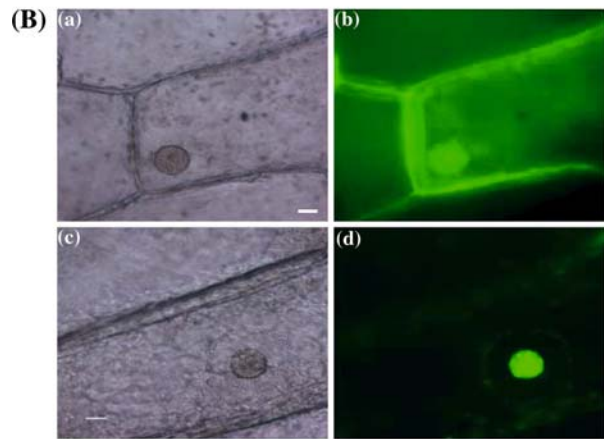
Figure 2. OsRad21-4 encodes an orthologue of yeast Rec8. (A) OsRad21-4 protein contains the domains and motifs essential to function of Rad21/Rec8 proteins. Pfam04825 and Pfam04824 are shown with single and double underlines, respectively. The potential nuclear localization signal, separase recognition sites and PEST motif are marked with bold, italic and shadowed fonts, respectively. (B) OsRad21-4 is a nucleus-localizing protein. Onion epidermal cells were infected by *Agrobacterium tumefaciens* containing the plasmid harboring a GFP coding sequence (A and B) or OsRad21-4::GFP fusion construct (C and D), These infected cells were observed by optical microscopy (A and C) or fluorescence microscopy with a FITC filter (B and D). GFP accumulated in the nucleus and cytoplasm (B). OsRad21-4::GFP fusion protein accumulated in the nucleus (D). Scale bar in (A) = 20 μm for (A)–(D). (C) Phylogenetic analysis revealed that OsRad21-4 was grouped with Rec8-like proteins from other species and formed a clade with Arabidopsis Syn1. The tree was derived from the multiple alignments of N-terminal regions of OsRad21-4 and other Rad21/Rec8 sequences with use of Clustal W plus a neighbor-joining feature with removal of most distance sequences. These sequences are shown as follows: OsRad21–1 and OsRad21-4 (this study, *Oryza sativa*, accession No. AY28893 and AY371049); Syn1, Syn2 and Syn3 (*Arabidopsis thaliana*, accession No. AF080619, AF281154 and AF281155); HsRad21 and HsRec8 (*Homo sapiens*, accession No. NM_006265 and NM_005132); MmRad21 and MmRec8 (*Mus muculus*, accession No. NP_033035 and AAF69524); CeRec8 (*Caenorhabditis elegans*, accession No. CAB05309); DmRad21 (*Drosophila melanogaster*, accession No. NM_143900); XRad21 (*Xenopus laevis*, accession No. AF051786); and SpRec8 (*Schizosaccharomyces pombe, accession* No. AB018077). Bootstrap values, evaluated for 100 bootstrap trails, are shown at branch points.

5.0–7.0 mm as F4. F1 flowers were at the stamen and carpel primordial formation stage, F2 at the premeiotic PMC stages, F3 at the meiotic PMC stage and F4 at the uninucleate pollen stage. As shown in Figure 3C, the transcript appeared to be accumulated at the F1 stage, increased to the highest level at the F2 stage, then decreased with proceeding meiosis (F3) and finally declined to a low level at the F4 stage. The transcript was undetectable in mature pollen grains. These results demonstrate that in developing flowers, *OsRad21-4* was expressed dominantly just before the premeiotic stage of PMCs.

Finally, *in situ* hybridization was performed to define which cells of flowers the gene was expressed in. We used DIG-labeled OsRad21-4 antisense and sense RNA probes (control) to probe cross-sections of flowers. In anthers, the greatest signal was detected in premeiotic PMCs (Figure 4A) and relatively strong signals in meiotic
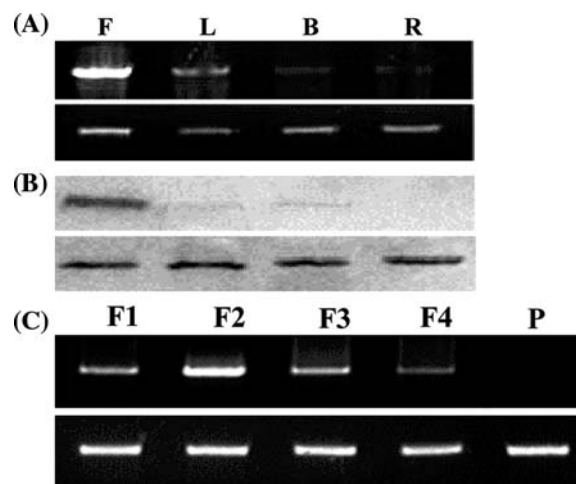
Figure 3. Accumulation patterns of OsRad21-4 mRNA and protein in different organs. (A) RT-PCR analyses of OsRad21-4 mRNA accumulation. PCR was performed with first-strand cDNAs synthesized with total RNA from flowers (F), leaves (L), buds (B) and roots (R), and gene-specific primers P9 and P10 (see Figure 1). PCR products were separated on 1% agarose gels. Top-panel, specificity of OsRad21-4 mRNA accumulation; Bottom, control with rice tubA mRNA. (B) Western blotting analyses of OsRad21-4 protein accumulation. Total proteins were extracted from flowers (F), leaves (L), buds (B) and roots (R), separated on 12% SDS-PAGE and then transferred to PVDF membrane. Immunoblotting involved use of a polycolonal antibody against Os-Rad21-4 (Top panel, the band size was ~67 kDa) or tubulin A (Bottom panel). (C) Developmental regulation of *OsRad21-4* expression in flowers, which were in carpel and stamen primordial formation stage (F1), premeiotic pollen mother cell (PMC) stage (F2), meiotic PMC stage (F3) or uninucleate microspore stage (F4), and mature pollen grains (P). RT-PCR involved use of total RNAs from these developing flowers and mature pollen grains, and the primer set P9/P10. Top panel, specificity of OsRad21-4 mRNA accumulation; Bottom, control with rice tubA mRNA.
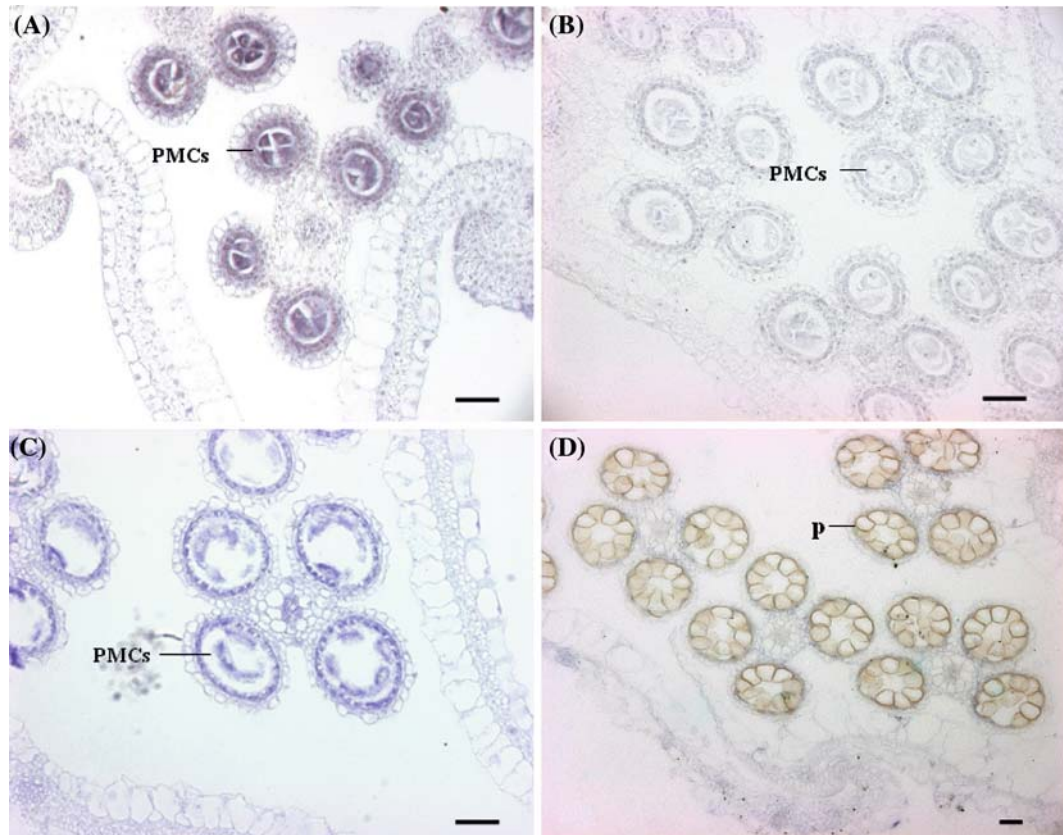
Figure 4. In situ hybridization analyses of OsRad21-4 mRNA in flowers. Traverse sections of flowers in premeiotic PMC stage (A and B), meiotic PMC stage (C). or uninucleate pollen stage (D) were hybridized with DIG-labeled antisense RNA (A, C and D) or sense RNA (B, control) probe. Signals were detected with an anti-DIG-antibody-conjugated alkaline phosphatase and visualized with the chromagenic substrates NBT and BCIP (Roche). PMCs, pollen mother cells; T, tapetum; P, uninucleate pollen. Bars in (A) = 20 μm for (A)–(C), and in (D) = 20 μm.

PMCs (Figure 4C) and tapetal cells (Figure 4A and C). No signal was detected in uninucleate pollen grains (Figure 4D) and other parts of anthers (Figure 4A, C and D). No signals occurred in other flower organs (lemma, palea) (Figure 4A, C and D). Sense probes did not detect signals in the flowers (Figure 4B). All these results gave a direct indication that this gene should function in premeiotic and meiotic PMCs, which is consistent with this notion that meiotic cohesion is established at the pre-meiotic S phase (Watanabe *et al.*, 2001).

Generation and screening of OsRad21-4 RNAi lines

RNA interference (RNAi) can specifically and efficiently result in degradation of endogenous target transcripts into $\sim$22-nt small RNA, and subsequent knockdown or knockout of the target gene, so it is a convenient tool of reverse genetics to study gene functions (Chuang and Meyerowitz, 2000; Wesley *et al.*, 2001). Therefore, RNAi was used to gain insight into the function of *OsRad21-4* in rice development. The RNAi construct pRAD21-4i was generated by inserting a 769-bp fragment spanning 468-1236 nt of OsRad21-4 cDNA, with no similarity to the 3 other *RAD21*-like genes of rice, into pWTC605 in the sense and antisense orientations separated by a spacer sequence (Figure 5A, also see Materials and methods). In pRAD21-4i, a CaMV35S promoter drove transcription of the sense::spacer::antisense fusion sequence.

After embryonic calli were infected with *A. tumefaciens* EHA105 carrying pRAD21-4i and
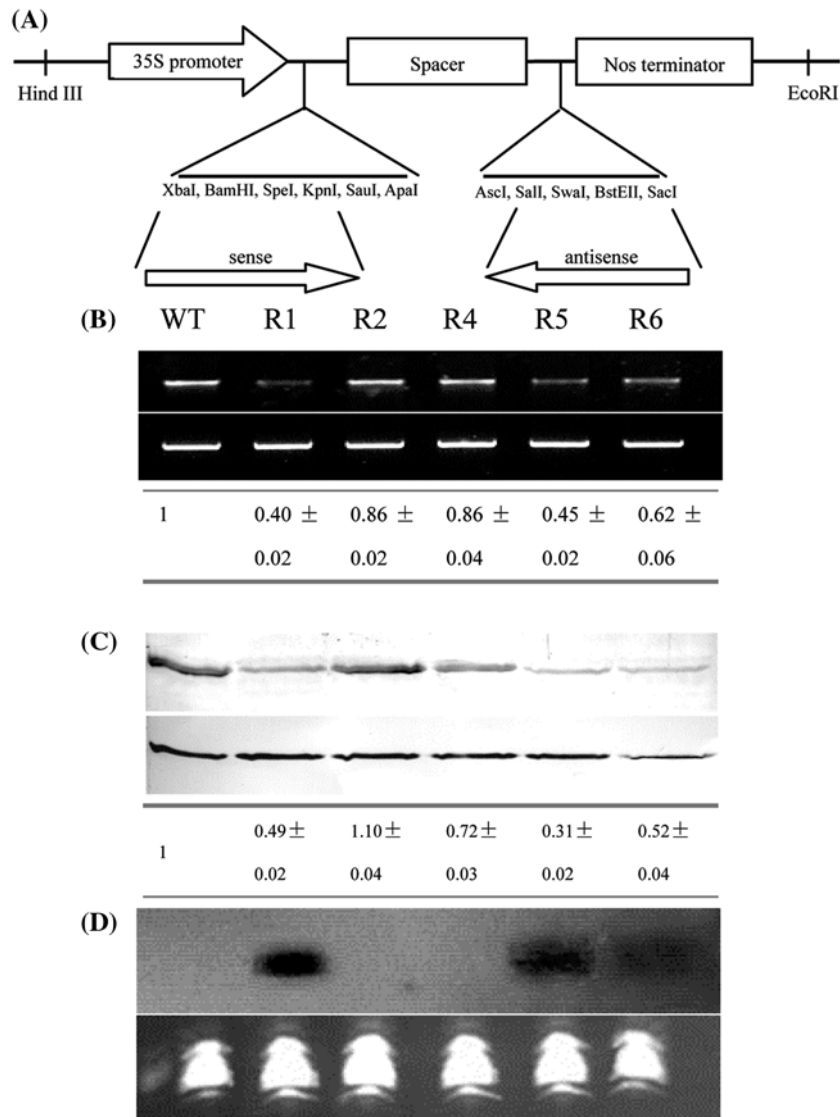
Figure 5. The presence of ~23 nt small RNAs correlates with decreased levels of OsRad21-4 transcript and protein in *OsRad21-4* RNAi lines. (A) A schematic picture of pRAD21-4i constructed by inserting a cDNA fragment of OsRad21-4 into pWTC605 at sense and antisense orientations, respectively. pWTC605 was constructed by inserting the shown construct into pCAMBIA1300 at *Eco*RI and *Hin*dIII sites (see Materials and methods). (B) Semi-quantitative RT-PCR analysis of OsRad21-4 mRNA extracted from flowers of independent transgenic lines R1, R2, R4, R5 and R6, and wild type (WT) with the primer set P9/P10, along with *tubA* as a constitutive control. Quantification of mRNA levels (ratios of normalized data for transgenic lines vs wild type [WT]) is listed below the picture. The data were means of triplicates and SDS are shown. (C) Western blot detection of OsRad21-4 protein from flowers of these lines. Tubulin protein was used as a constitutive control. Quantification of protein levels (ratios of normalized data for transgenic lines versus WT) is listed below the picture. The data are means of triplicates and SDs are shown. (D) Northern blotting analysis of OsRad21-4-specific small RNA in these lines (see Materials and methods). Top panel, ~23-nt small RNA specific to OsRad21-4. Bottom, ethidium bromide-stained gel showed equal amount of low-molecular-weight RNA loaded.

subsequently selected on hygromycin-selection medium, 12 independent T_0 transformants generated from hygromycin-resistant independent calli were obtained and planted under standard growth conditions. PCR analysis of insertion of the transgene in the genome with use of the primer pair localized at the spacer and sense or antisense sequences of this construct revealed that the

predicted ~870-bp fragment was detected in all the transgenic lines but not in the wild-type control. Compared with the wild type, which had a >98% seed setting rate, 9 of the 12 lines had a heavily decreased seed setting rate (<10% in 5 lines; < 40% in 4 lines) and the other three lines appeared to be less affected in seed setting rate (>60%). The phenotypes of seed production in each line was stable in their regenerated plants (termed R). These results suggest that *OsRad21-4* is involved in rice fertility. Except for the affected fertility, these RNAi lines did not display other abnormal phenotypes as compared to the wild type.

Moreover, 5 lines including 1 medium sterile phenotype (line 4, 37.9% setting rate), 3 severely sterile phenotype (line 1, 9.7%; line 5, 5.5%; line 6, 29%) and 1 low sterile phenotype (line 2, 61%) were subjected to insertion copy examination by Southern blotting with use of a ^{32}P-labeled DNA fragment of the selectable marker hygromycin gene in the RNAi construct, along with the wild type as a control. Two insertions occurred in lines 1, 2 and 6, 1 in lines 4 and 5, and none in the wild-type control (data not shown). We found no relation between the insertion number of the transgene and seed setting rate. The uncertainty reflects significant variation of the transgene expression level, which may be affected by many factors, including integration sites and rearrangement (Kohli *et al.*, 2003). Therefore, the three lines were used for further analysis.

Knockdown of OsRad21-4 mRNA and protein in RNAi plants is related to their sterility

To investigate whether the sterility phenotype correlates to RNAi-mediated knockdown of this target mRNA, endogenous OsRad21-4 transcripts were determined by semi-quantitative RT-PCR with use of RNAs prepared from flowers of lines R1, R2, R4, R5 and R6, as well as the wild type, with tubA mRNA as a control to indicate that equal amount of RNAs were used in the RT-PCR experiments. Compared with the wild type, R1, R5 and R6 contained greatly down-regulated OsRad21-4 transcripts. The level of OsRad21-4 transcripts in R2 and R4 appeared to be unaffected (Figure 5B). Next, we examined the OsRad21-4 protein in these lines by western blot analysis. The protein level in R1, R5 and R6 was decreased by 50.2%, 69.5% and 48%, respectively,

and in R4 by 27.5%, as compared with that of the wild type. R2 had a protein level similar to that of the wild type (Figure 5C). These results indicate that deficiency of OsRad21-4 mRNA and protein in R1, R4, R5 and R6 is associated with their sterile phenotype. R2, though containing an insertion of the transgene, had unaffected mRNA and protein levels, and thus its seed setting rate was less affected as compared with the wild type, so for further analysis, it was also used as a transformed control, referred as [R2 hyg$^+$] control below, with the wild-type control.

To further estimate whether the decrease in endogenous OsRad21-4 mRNA and protein levels resulted from RNA interference mediated by the introduced RNAi construct, low-molecular-weight RNAs were fractioned from RNA samples prepared from flowers of OsRad21-4-deficient lines R1, R4, R5 and R6, as well as wild-type and [R2 hyg$^+$] controls. Results of northern hybridization with an OsRad21-4 cDNA probe demonstrated that the target cDNA-specific small RNA of ~23 nt was detectable in R1, R5 and R6 and undetectable in R4 and controls (Figure 5D). The difficulty in detecting a 23-nt RNA fragment in R4 may result from the low level of fragments generated in this line, which is consistent with the mRNA and protein expression being not as severely disrupted as in R1, R5 and R6. Clearly, generation of the gene-specific small RNAs led to knockdown of OsRad21-4 mRNA and protein in these deficient lines. So the RNAi-mediated OsRad21-4 deficiency at the mRNA and protein levels in these lines is correlated with their sterility phenotype.

Aborted pollen is associated with the decreased setting rate in RNAi lines

Because pollen is a key regulator of successful fertilization in sexual plants, we compared the pollen development of OsRad21-4-deficient lines R1, R5 and R6 with wild-type and [R2 hyg$^+$] controls. Mature anthers from the deficient lines did not differ in morphology from those of controls, but the former contained a markedly decreased amount of pollen grains than the latter. And each anther of the deficient line R5 had only 31%, on average, of the pollen grain amount observed in controls (counted pollen grains using a hematocyte arithmometer, the data is estimated

from 25 anthers from 25 independent flowers for each line) (Figure 6A and B).

In a I$_2$-KI staining assay, ~98% of pollen grains ($n = 1862$) from the wild-type control were round and had a uniform size, with a dark blue–black reaction (Figure 6C). In contrast, pollen grains of the deficient lines, although having a high proportion of I$_2$-KI reaction (~89%, $n = 1043$), were variable in size and shape; ~30% were much smaller or larger than normal pollen grains, 19% were empty, shrunken and pear-shaped and less than 45% had a normal size (Figure 6D). Furthermore, we examined pollen viability using 2, 3, 5-triphenyltetrazolium chloride (TTC) staining, which can be reduced to a red product by NADPH from the redox reaction of respiration metabolism occurring in pollen grains when they are in a rehydration environment. In this assay, only ~10% of pollen grains ($n = 932$) from line R5 was found to be "viable" (red) and the others are "nonviable" (yellow) (Figure 6F), and a similar situation was observed with line R1. The proportion of viable pollen grains was ~45% in line R4, whereas ~90% of pollen grains ($n = 1743$) were viable in controls (Figure 6E). Moreover, when the incubation time in TTC staining solution was prolonged to 2 h, ~15% of pollen grains from the deficient lines burst, but none did from the controls. These results clearly suggest that sterility of the deficient lines is mainly derived from abnormal pollen development.

OsRad21-4 is required for meiosis in rice

To estimate whether a decreased pollen amount and aborted pollen grains in the OsRad21-4-deficient
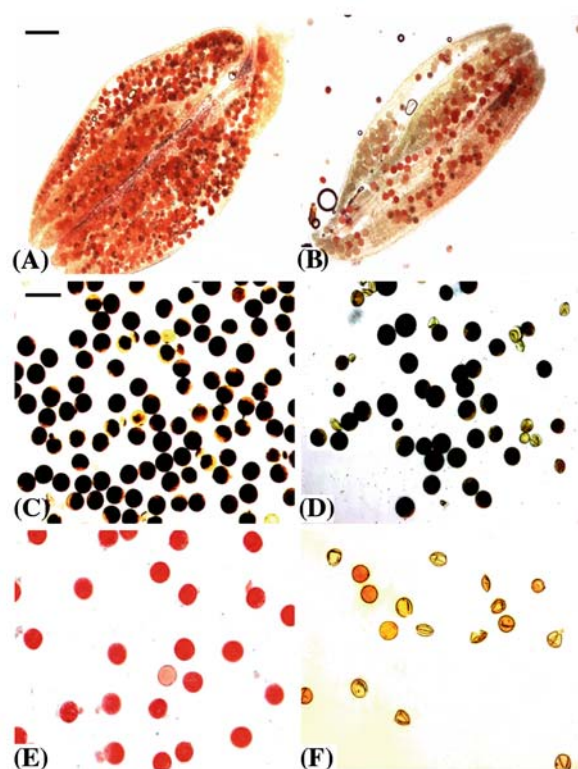
Figure 6. Pollen viability of OsRad21-4-deficient lines was severely affected. Intact anthers in wild type (A) and deficient lines (B) were stained with TTC solution and spread gently, showing that the deficient-line anthers contained a decreased amount of pollen grains as compared with wild type anthers. Viability of mature pollen grains in wild type (C and E) and deficient lines (D and F) were examined on I$_2$-KI (C and D) or TTC (E and F) staining. Pollen grains filled with starch granule showed dark blue, but those with little or no starch showed weak yellow during I$_2$-KI staining. Viable pollen grains showed red, with yellow for nonviable ones in TTC staining. Scale bars in (A) = 250 μm for (A) and (B), and in (C) = 80 μm for (C)–(F).

546

lines resulted from abnormal male meiotic behaviors, we prepared DAPI-stained chromosome spreads of male meiocytes of the deficient lines R1 and R5, along with wild-type and [R2 hyg$^+$] controls (more than 100 male meiocytes from 5 independent anthers at each stage for each line). In control plants, chromosomes in leptonema cells appeared as thin threads that looped out of dense syniizetic knots (Figure 7A). Homologous chromosomes begin to associate side by side at zygonema (Figure 7B), and fully synapse and condense into thick threads at pachynema (Figure 7C). After fully synapsed homologues further condense and synapsis is released at the arms at diplonema (Figure 7D), 12 X-formed bivalents became tightly condensed at diakinesis (Figure 7E). Afterwards, highly condensed 12 bivalents are aligned on equator plates at metaphase I (Figure 7F) and undergo reductional division at anaphase I (Figure 7G and H), generating dyads (Figure 7I and J). During meiosis I, the 2 daughter cells divide simultaneously with 2 parallel orientations of spindles, generating tetrads (Figure 7K and L).

As shown in Figure 8, the first detectable defects appeared in leptonema microsporocytes from the deficient lines (data are shown for R5 only). Approximately 35.6% of these cells ($n = 342$) contained very "sticky" chromosomes, which were difficult to spread. These chromosomes were observed as a compact entangled mass with dark staining (Figure 8A) and rarely appeared as thin threads in control plants (Figure 7A). At approximate zygonema, chromatins appeared unevenly condensed, with most regions highly condensed into agglomerations interrupted by dispersed threads (Figure 8B). Thread-like chromosomes, which were typical in control plants, were rarely observed. During pachynema, completely synapsed homologues in control plants condensed into a thick thread-like structure (Figure 7C), whereas at approximate pachynema in the deficient lines, the normal appearance of thick-threads was seldom observed; the abnormal thick thread-like chromosomes displayed separated telomeric regions, while their central regions seemed to
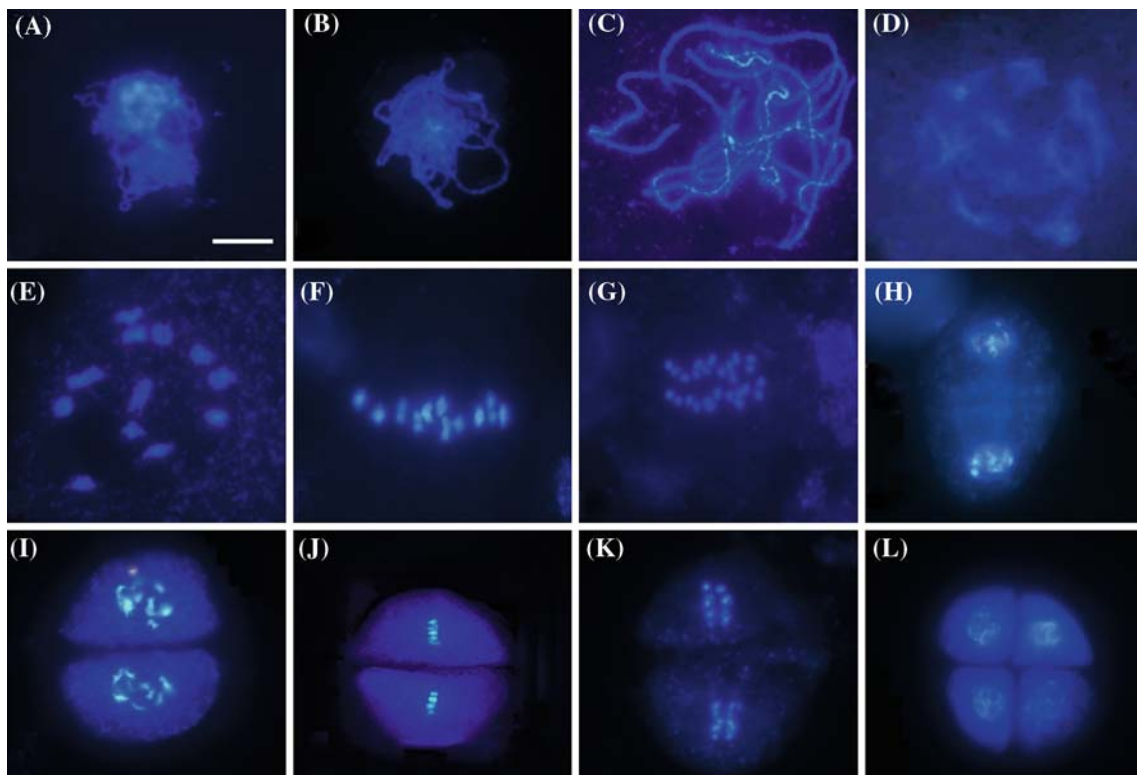
Figure 7. DAPI-stained chromosome spreads of male meiocytes in wild type. (A) leptonema; (B) zygonema; (C) pachynema; (D) diplonema; (E) late diakinesis; (F) metaphase I; (G) anaphase I; (H) dyad; (I) prophase II; (J) metaphase II; (K) anaphase II; (L) tetrad. Bar in (A) = 20 μm for (A)–(L).
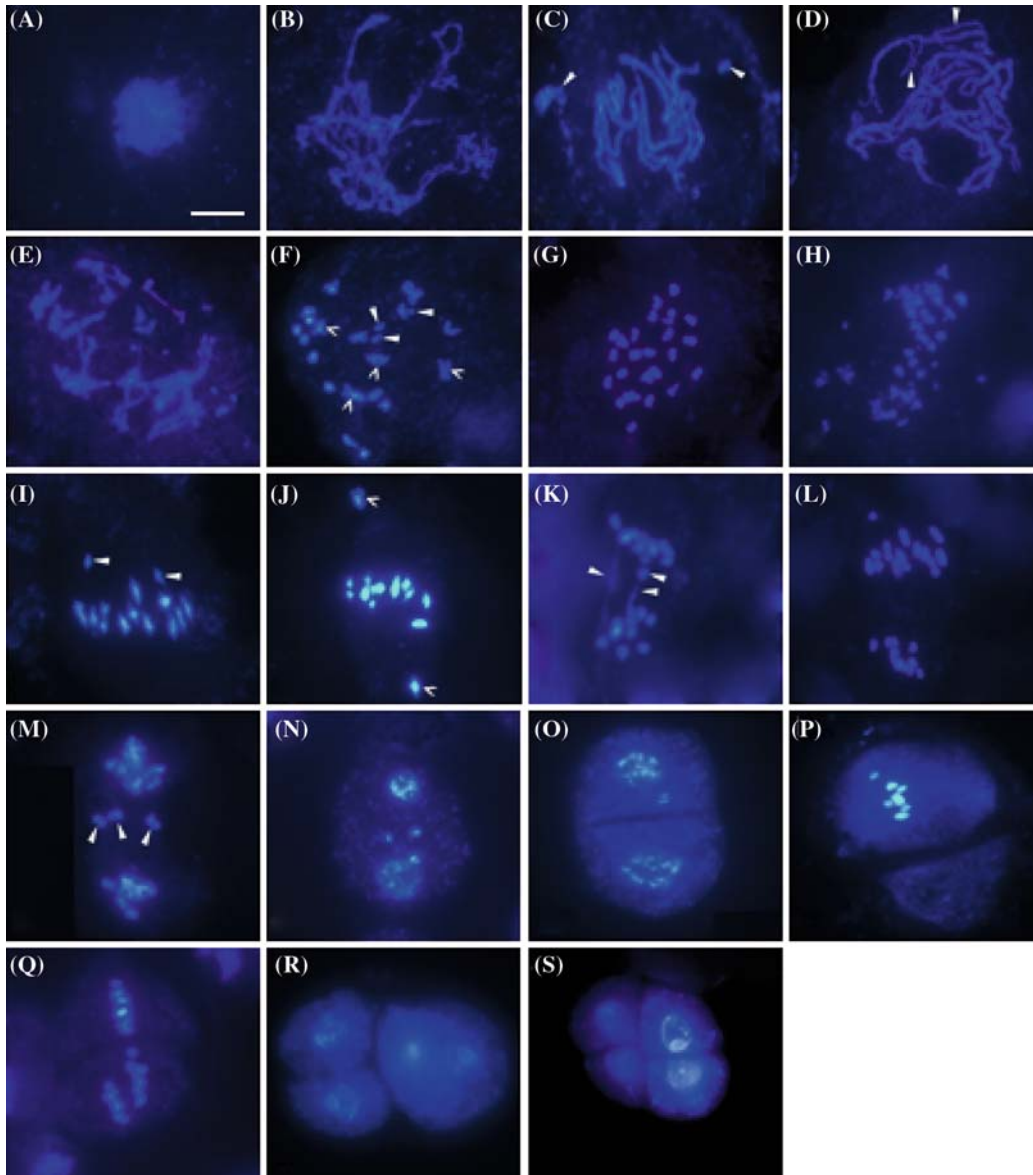
Figure 8. Abnormal meiotic chromosome behavior in microsporocytes of OsRad21-4-deficient lines. Meiosis chromosome spreads were prepared from fixed anthers from the deficient lines (R1 and R5, data are shown only for R5). (A) leptonema; chromatins were compacted into a entangled mass. (B) zygonema; chromosomes showed defects in condensation, with most regions being highly condensed in agglomeration. (C) and (D) pachynema, chromosomes were highly condensed compared with those of the wild type and unsynapsed homologues, with detached regions distal to centromeres and chromosome fragments visible (arrows); (E) diplonema; homologues precociously segregated into univalents. (F) diakinesis; univalent (not marked), bivalents (concaved arrows) and chromosome fragments (arrows) are visible. (G) late diakinesis; homologues precociously segregated into 24 univalents. (H) late diakinesis; ∼50 stained bodies, reflecting severe chromosome fragmentation. (I) and (J) metaphase I; chromosomes (arrows) did not align on equator. (K) anaphase I; chromosome bridging was formed by lagging chromosomes linking two segregating groups of chromosomes (arrows). (L) anaphase I; chromosomes segregated randomly. (M) telophase I; chromosomes cannot be segregated into each pole (arrows). (N) dyad with lost chromosomes and unequal nuclei. (O) dyad with 1 cell having 2 unequal nuclei. (P) dyad with unequal nuclei and cytoplasm. (Q) metaphase II, 2 daughters lost synchronization to initiate transition of metaphase II to anaphase II. (R) tetrad stage; misorientation of spindles in 2 daughters resulted in cell division occurring in 1 daughter but not the other. (S) tetrad stage; 4 cells with unequal cytoplasm and chromosome complements. Bar in (A) = 20 μm for (A)–(S).

be attached (Figure 8C and D), and some chromosome fragments were also detected (Figure 8C). Furthermore, precocious segregation of homologues were detected at approximate diplonema, where chromosomes appeared mainly as univalents (Figure 8E) instead of as ''X''-formed bivalents observed in control plants (Figure 7D), and chromosome fragments were visible. Therefore, at approximate diakinesis, affected meiocytes contained a varied number of univalents. A total of 16.9% of these diakinesis meiocytes ($n = 237$) contained a mixture of bivalents and univalents with several chromosome fragments as judged by their morphology (Figure 8F), 2.1% had 24 univalents (Figure 8G) and 3% were occupied mainly by chromosome fragments because they appeared as small dots beside bivalents and univalents (Figure 8).

Obviously, the precociously released univalents and fragmented chromosomes in the deficient lines led to improper chromosome alignment on the equator at approximate metaphase I (Figure 8I and J). Furthermore, the impaired anaphase I cells showed unequal chromosome separation (Figure 8L) and several lagging chromosomes (Figure 8M). Interestingly, 11.2% of anaphase I meiocytes ($n = 107$) showed a bridge between 2 segregating groups of chromosomes (Figure 8K). Finally, meiosis I gave rise to aberrant dyads with unequal nuclei and/or cell size (Figure 8N–P). Micronuclei or nuclei-losing cells were frequently observed (Figure 8N–P).

During meiosis II, only limited microsporocytes were observed in anthers of the deficient lines, possibly because most meiocytes died of abnormal meiosis I. Before telophase II, an obvious abnormality observed was the inability of 2 daughter cells (13%, $n = 153$) to initiate transition from metaphase II to anaphase II synchronously (Figure 8Q). Finally, asymmetric ''tetrads'' (43%, $n = 173$) containing 3 cells, with 1 having dinuclei, or 4 cells with unequal cell size and chromosome complement appeared (Figure 8R and S).

OsRad21-4 deficiency appeared to disrupt homologous pairing and sister arm cohesion

Furthermore, we examined sister chromatid cohesion and homologous pairing using a 25S rDNA probe (Figure 9), which corresponds to the short-arm end of chromosome 9 in *japonica* rice (Shish-

ido *et al.*, 2000). In wild-type plants, about 56% of leptonema male meiocytes ($n = 50$) have 1 FISH signal and the others 2 signals, the percentage of the cells with 1 FISH signals was increased to 82% at zygonema. No cells were detected to show more than 2 signals at the two stages. At pachynema, nearly 100% of the mal meiocytes had 1 FISH signal. But in OsRad21-4-deficient lines (data are shown for R5 only), only 28%, 40% and 64% of male meiocytes had 1 FISH signal at these three corresponding stages. At each corresponding stage, the cells with more than 2 FISH signals were observed (Figure 9). Importantly, at approximate pachynema, some male meiocytes still had 2 or more FISH signals. This suggests that knockdown of OsRad21-4 affected both sister chromatid arm cohesion, and homologous chromosome pairing and synapsis.

Cohesion and pairing of centromeric regions were also investigated by use of the centromere probe CentO (Figure 10), which can recognize all chromosome centromeres in *japonica* rice (Cheng *et al.*, 2002). In wild-type plants, from leptonema to zygonema, 8–12 centromere signals were observed in 52% and 78% of examined male meiocytes ($n = 50$), respectively, with the remaining cells having 13–24 signals. And at pachynema, 100% of the cells had 8–12 signals. In contrast, in the deficient lines, the number of these cells with 8–12 signals was 22% and 38% at the corresponding leptonema and zygonema, respectively, and the others had 13–24 signals. At approximate pachynema, only 82% of the cells had 8–12 signals and the others still showed 13–24 signals. However, no meiocytes examined contained more than 24 centromere signals in the deficient lines. This suggests that centromeric cohesion of sister chromatids may be intact, but pairing of some homologous chromosomes was disrupted in the deficient lines.

Discussion

Our results from the present and a previous (Zhang *et al.*, 2004) study have demonstrated that the rice genome encodes 4 Rad21-like proteins, which share a limited similarity bweteen their N- and C-domain regions. Of them, OsRad21-4 is closest to the Rec8 proteins of the Rec8/Rad21 family. Furthermore, we obtained OsRad21-4-deficient
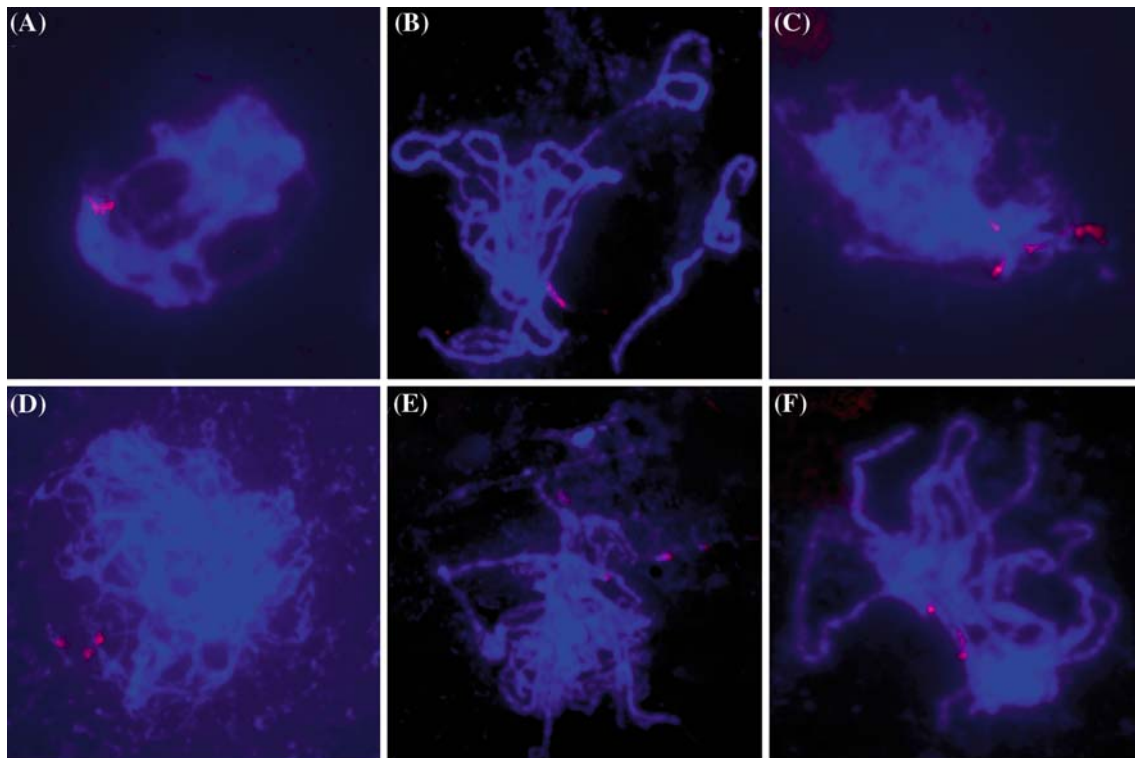
	1 FISH locus	2 FISH loci	3-4 FISH loci
leptotene	28% (56%)	44% (44%)	28%
zygotene	40% (82%)	34% (18%)	26%
pachytene	64% (100%)	18%	18%

Figure 9. Fluorescence *in situ* hybridization (FISH) using a probe of 25S rDNA in wild type (A, B) and OsRad21-4-deficient (C–F) plant male meiocytes. The probe was labeled with digoxigenin-labeled dUTP and detected with rhodamin-conjugated anti-digoxigenin antibody (red). Chromosomes were counterstained with DAPI (blue). (A, C) leptotene; (B) pachytene; (D) zygotene; (E) early pachytene; (F) pachytene. The experimental data were summaried and listed below the picture. The data in the bracket were from wild type plants, and the others from the deficient plants. $n = 50$.

lines mediated by RNAi and identified the function of this protein in meiosis by monitoring meiotic chromosome behaviors of male meiocytes of these deficient lines.

OsRad21-4 is required for pairing and segregation

Aberrant phenotypes of OsRad21-4-deficient plants were first detectable at approximate laptonema. Tangled chromosomes were observed through leptonema to zygonema. Soon after, the tangled structure could be partially relieved, and subsequent stages of prophase I were distinguishable, but the chromosome appearance was abnormal. At approximate pachynema, the abnormal thick thread-like chromosomes showed obviously separated telomeric regions. In addition, at this stage in the deficient lines, 36% of male meiocytes had 2 or more 25S rDNA loci, which is close to the short arm of chromosome 9 (Shishido *et al.*, 2000), and 18% had 13–24 centromere signals. This indicated that OsRad21-4 deficient lines were defective in homologous pairing and possibly in synapsis. Thus, we can conclude that OsRad21-4 is required for homologous pairing. A similar function has been identified for Rec8 protein from fission and budding yeast, and for its homologs from *C. elegans* and Arabidopsis by mutation analysis (Klein *et al.*, 1999; Watanabe and Nurse, 1999; Pasierbek *et al.*, 2001; Cai *et al.*, 2003) and inferred for rat Rec8 protein from chromosome localization analysis (Eijpe *et al.*, 2003), which
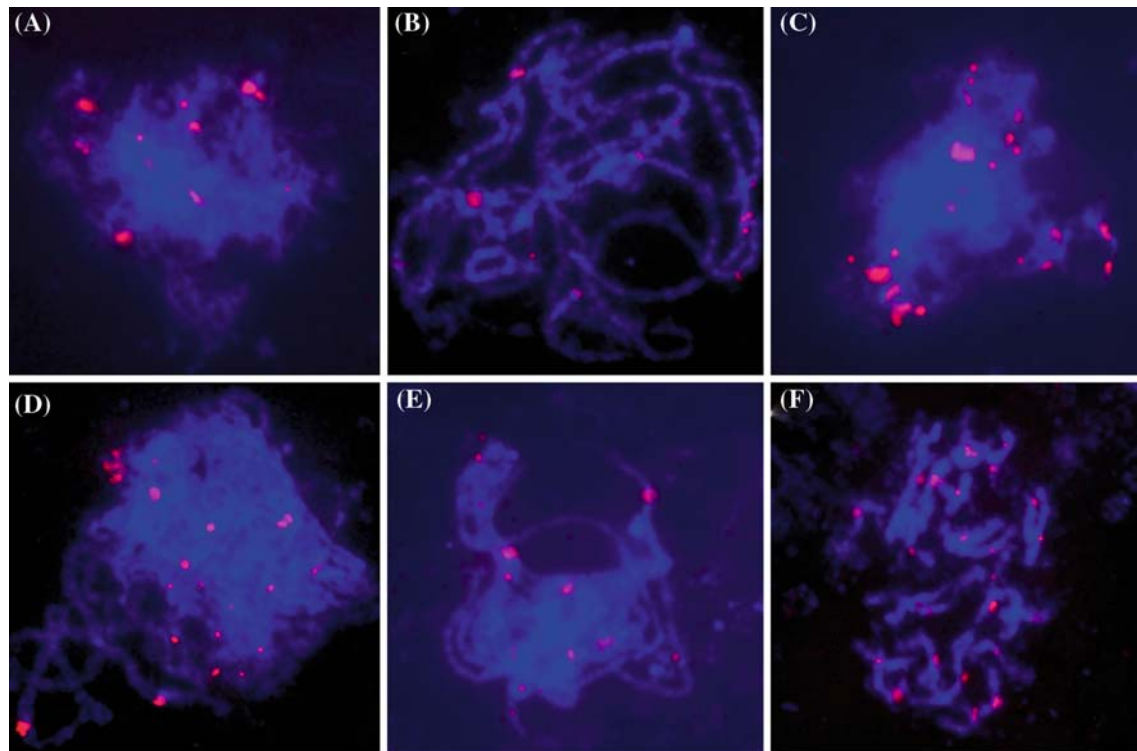
	8-12 FISH loci	13-24 FISH loci
leptotene	22% (52%)	78% (48%)
zygotene	38% (78%)	62% (22%)
pachytene	82% (100%)	18%

Figure 10. FISH of the centromere probe CentO in wild type (A, B) and OsRad21-4 deficient (C–F) plant male meiocytes. CentO was labeled with digoxigenin-labeled dUTP and detected with rhodamin-conjugated anti-digoxigenin antibody (red). Chromosomes were counterstained with DAPI (blue). (A, C) leptotene; (B, D) zygotene; (E) pachytene; (F) late diplotene. The experimental data were summarised and listed below the picture. The data in the bracket were from wild type plants, and the others from the deficient plants. $n = 50$.

suggests that the general function of the meiotic cohesin protein is highly conserved in different organisms.

However, OsRad21-4-deficient lines showed precocious segregation of homologues but not sister chromatids through prophase I. FISH experiments revealed that, from approximately zygonema to pachynema, some meiocytes displayed 3–4 loci of 25S rDNA, while no cells had more than 24 centromere signals. These results demonstrate that OsRad21-4 deficiency impaired sister-arm cohesion but, to a lesser extent or not at all, their centromere cohesion. So in rice, Os-Rad21-4 might be responsible mainly for sister chromatid-arm cohesion and to a lesser extent or not at all for centromere cohesion. Interestingly, a similar phenotype was observed in the Arabidopsis *syn1* mutant, which showed defective cohesion at sister arms but not at centromeres throughout prophase I (Cai *et al.*, 2003). Because the Arabidopsis genome has 3 *RAD21*-like genes (Dong *et al.*, 2001) and rice contains 4 *RAD21*-like genes, other Rad21-like proteins in each genome may play roles in holding sister centromeres. In fact, phylogenetic analysis has shown that rice Os-Rad21–2 as well as Arabidopsis Syn2 could grouped with other known Rec8 proteins, including OsRad21-4 and Syn1 (Figure 2C). Alternatively, the possibility that residual OsRad21-4 protein in the deficient lines is responsible for cohesion at sister centromeres seems unlikely because we did not find any male meiocytes

exhibiting premature segregation of sister chromatids through meiosis I.

By contrast, in Rec8-deleted *C. elegans* mediated by RNAi, most sister chromatids are completely disconnected at diakinesis I (Pasierbek *et al.*, 2001) although an additional 3 Rad21-like proteins are encoded in this genome. Budding and fission yeast carrying a *rec8* mutation showed most or all sister chromatids preciously segregated during meiosis I (Klein *et al.*, 1999; Watanabe and Nurse, 1999). The phenotypic difference between higher plants and the above analyzed eukaryotes should reflect a modified function of the meiotic cohesin in plants. Further efforts need to identify how plants differentially regulate meiotic cohesion at sister arms and at centromeres.

OsRad21-4 is required for chromosome condensation

Chromosome condensation contributes to chromosome longitudinal compaction by trapping supercoils with a defined chirality, chromosome individualization and the resolution of chromosomes into distinct spatial domains (Nasmyth, 2002), thus being essential to chromosome segregation. Our results provide clues suggesting that the meiotic cohesin protein Rec8 (here OsRad21-4) is implicated in condensation, as evidenced by the following phenotypes: (1) chromosomes at approximate leptonema in OsRad21-4-deficient lines appeared to be compacted into an entangled mass (Figure 8A) and were rarely observed as thin threads present in wild-type meiocytes (Figure 7A); (2) chromosomes at approximate zygonema showed highly condensed agglomeration (Figure 8B) instead of a clear thread-like structure typical of chromatins from wild-type meiocytes (Figure 7B); (3) pachynema chromosomes seemed to be compacted more severely in the deficient lines (Figure 8C and D) than those in wild type (Figure 7C); and (4) importantly, anaphase I cells of the deficient lines had chromosome bridging (Figure 8K), which is a typical phenotype of aberrant condensation in mitotic cells of all observed organisms to date (Yu and Koshland *et al.* 2003). These discoveries, combined with the first 2 phenotypes also observed in the Arabidopsis *syn1* mutant (Bai *et al.*, 1999; Cai *et al.*, 2003), indicate that meiotic cohesin Rec8 proteins in

higher plants appear to be required for efficient chromosome condensation.

However, the phenotypes have not been detected in the other *rec8* mutants analyzed to date. Rec8-deleted *C. elegans* by RNAi (Pasierbek *et al.*, 2001) and the fission yeast *rec8* mutant did not show chromosome over-condensation (Watanabe and Nurse 1999). In contrast, the budding yeast *rec8* mutant lost partial ability to condense chromosomes (Klein *et al.*, 1999), sharing a similar phenotype with its mitotic counterpart *scc1/mcd1* mutant, which generated decondensed chromosomes (Lavoie *et al.*, 2002). The phenotypic differences raise a possibility that higher plants, possibly mammals, employ a mechanism, different to that operating in *C. elegans* and yeast, to handle the interplay of cohesin and condensin to regulate meiotic chromosome compact and individualization because of their complex chromosome structure, such as repetitive DNA elements, which in rice constitute at least 50% of the genome (Eckardt, 2000).

In budding yeast, the *rec8* mutation did not affect loading of condensin proteins to meiotic chromosomes and vice versa, similar to mitotic *scc1/mcd1* mutation (Lavoie *et al.*, 2002; Yu and Koshland, 2003). But in the absence of functional Mcd1, chromatin-binding condensin fails to promote condensation (Lavoie *et al.*, 2002). Mitotic cohesin in budding yeast, proposed as a *cis* determinant, might dictate the condensin binding sites on chromosomes and cohesin deficiency might lead to inability of condensin to bind the specific regions (Lavoie *et al.*, 2002). However, little is known about how meiotic cohesin Rec8 functions in condensation now.

Possible link between Rec8 proteins and chromosome fragmentation in higher eukaryotes

OsRad21-4 deficiency also led to meiotic chromosome fragmentation. The abnormal chromosome behavior has been observed in the Rec8-deleted *C. elegans* (Pasierbek *et al.*, 2001) and Arabidopsis *syn1* mutant (Bai, *et al.*, 1999; Cai *et al.*, 2003) but not in fission and budding yeast carrying the *rec8* mutation (Klein *et al.*, 1999; Watanabe and Nurse, 1999), seemingly related to an increased chromosome size of these higher organisms. Of them, *C. elegans* has a mean chromosome size of 16.7 Mb, Arabidopsis 20 Mb and rice 35.8 Mb,

552

compared to the mean 4.7-Mb and 0.75-Mb chromosome size of fission and budding yeast, respectively. Condensation contributes to chromosome compaction and is essential for sister chromatid disentanglement (Kitajima *et al.*, 2003a, b). A recent study of budding yeast revealed that mutation in meiotic condensin proteins led to chromosome fragmentation (Yu and Koshland, 2003). Indeed, rice OsRad21-4-deficient and Arabidopsis *syn1* mutants showed strong over-condensation of chromosomes. Chromosome fragments in OsRad21-4-deficient lines were first observed at approximate pachynema (Figure 8C), before the end of recombination. This observation implies that OsRad21-4 deficiency-mediated abnormal condensation in rice is involved in the chromosome fragmentation. But exceptionally, no defect in meiotic condensation was observed in Rec8-deleted *C. elegans* (Pasierbek *et al.*, 2001).

Therefore, an alternative possibility cannot be excluded now that the fragments could result from unrepaired double-strand breaks (DSBs) in OsRad21-4-deficient mutants. For this explanation, an indirect evidence is that Rec8-deleted *C. elegans* carrying a *spoll* mutation did not generate chromosome fragments (Pasierbek *et al.*, 2001). Inconsistently, budding yeast *rec8* mutants have no chromosome fragmentation, although the proteins seem to be necessary for efficient recombination between homologs (Klein *et al.*, 1999). Rec8 in fission yeast is not required for repair of meiotic DSBs (for review, see Davis and Smith, 2001). In fact, the worm along with *Drosophilia* represents a exceptional meiosis model (Dernburg *et al.*, 1998; McKim *et al.*, 1998; Pasierbek *et al.*, 2001) and exhibits a marked difference in chromosome behavior of meiosis prophase I from yeast (Zickler and Kleckner, 1999), higher plants (Grelon *et al.*, 2001; Li *et al*, 2005; Ma 2005) and vertebrates (Baudat *et al.*, 2000) (also see ''introduction''). So this explanation is devoid of additional evidence.

In summary, OsRad21-4-deficient plants mediated by RNAi showed multiple aberrant events at meiosis prophase I, including over-condensation of chromosomes, precocious segregation of homologues and chromosome fragmentation. But precocious release of sister chromatids at prophase I was not observed in the deficiency lines. FISH experiments revealed that deficiency of OsRad21-4 appeared to disrupt homologous pairing and at sister arm cohesion, but not centromere cohesion.

Furthermore, appearance of micronuclei and/or undetached dinuclei-containing spores and unequal cell division at anaphase I and II in the deficient plants were similar to those reported in mutants of genes related to other early events of meiosis prophase I (Ma, 2005), such as *PAIR1* in rice for pairing (Nonomura *et al.*, 2004) and *PHS1* in maize for pairing, recombination and synapsis (Pawlowski *et al.*, 2004), suggesting possible interaction of early events of prophase I.

References

Bai, X., Peirsion, B.N., Dong, F., Cai., X. and Makaroff, C.A. 1999. Isolation and characterization of *SYN1*, a *RAD21*-like gene essential for meiosis in Arabidopsis. Plant Cell 11: 417–430.

Baudat, F., Manova, K., Yuen, J.P., Jasin, M. and Keeney, S. 2000. Chromosome synapsis defects and sexually dimorphic meiotic progression in mice lacking Spo11. Mol. Cell 6: 989–998.

Bhatt, A.M., Lister, C., Page, T., Fransz, P., Findlay, K., Jones, G.H., Dickinson, H.G. and Dean, C. 1999. The *DIF1* gene of Arabidopsis is required for meiotic chromosome segregation and belongs to the *REC8/RAD21* cohesin gene family. Plant J. 19: 463–472.

Birkenbihl, R.P. and Subramani, S. 1992. Cloning and characterization of *rad21* an essential gene of *Schizosaccharomyces pombe* involved in DNA double-strand-break repair. Nucl. Acids Res. 20: 6605–6611.

Buonomo, S.B.C., Clyne, R.K., Fuchs, J., Loidl, J., Uhlmann, F. and Nasmyth, K. 2000. Disjunction of homologous chromosomes in meiosis I depends on proteolytic cleavage of the meiotic cohesion Rec8 by separin. Cell 103: 387–398.

Cai, X., Dong, F., Edelmann, R.E. and Makaroff, C.A. 2003. The Arabidopsis SYN1 cohesin protein is required for sister chromatid arm cohesion and homologous chromosome pairing. J. Cell. Sci. 116: 2999–3007.

Chen, C., Xu, Y., Ma, H. and Chong, K. 2005. Cell biological characterization of male meiosis and pollen development in rice. J. Integrative Plant Biol. 47: 734–744.

Cheng, Z., Dong, F., Langdon, T., Ouyang, S., Buell, C.R., Gu, M., Blattner, F.R. and Jiang, J. 2002. Functional Rice Centromeres Are Marked by a Satellite Repeat and a

Centromere-Specific Retrotransposon. Plant Cell 14: 1691–1704.

Chuang, C.F. and Meyerowitz, E.M. 2000. Specific and heritable genetic interference by double-stranded RNA in *Arabidopsis thaliana* . Proc. Natl. Acad. Sci. USA 97: 4985–4990.

Davis, L. and Smith, G. 2001. Meiotic recombination and chromosome segregation in *Schizosaccharomyces pombe* . Proc. Natl. Acad. Sci. USA 98: 8395–8402.

Dernberg, A.F., McDonald, K., Moulder, G., Barstead, R., Dresser, M. and Villeneuve, A.M. 1998. Meiotic recombination in *C. elegans* initiates by a conserved mechanism and is dispensable for homologous chromosome synapsis. Cell 94: 387–398.

Ding, Z.J., Wu, X.H. and Wang, T. 2002. The rice tapetum-specific gene *RA39* encodes a type I ribosome-inactivating protein. Sex. Plant Reprod. 15: 205–212.

Dong, F., Cai, X. and Makaroff, C.A. 2001. Cloning and characterization of two Arabidopsis genes that belong to the RAD21/REC8 family of chromosome cohesin proteins. Gene 271: 99–108.

Eckardt, N.A. 2000. sequencing the rice genome. Plant Cell 12: 2011–2017.

Eijpe, M., Offenberg, H., Jessberger, R., Revenkova, E. and Heyting, C. 2003. Meiotic cohesin REC8 marks the axial elements of rat synaptonemal complexes before cohesins SMC1beta and SMC3. J. Cell. Biol. 160: 657–670.

Gruber, S., Haering, C.H. and Nasmyth, K. 2003. Chromosomal cohesin forms a ring. Cell 112: 765–777.

Grelon, M., Vezon, D., Gendrot, G. and Pelletier, G. 2001. *AtSPO11-1* is necessary for efficient meiotic recombination in plants. EMBO J. 20: 589–600.

Guacci, V., Koshland, D. and Strunnikov, A. 1997. A direct link between sister chromatid cohesion and chromosome condensation revealed through the analysis of MCD1 in *S. cerevisiae* . Cell 91: 47–57.

Hamilton, A.J. and Baulcombe, D.C. 1999. A species of small antisense RNA in posttranscriptional gene silencing in plants. Science 286: 950–952.

Hanly, W.C., Artwohl, J.E. and Bennett, B.T. 1995. Review of polyclonal antibody production in mammals and poultry. ILAR J. 37: 93–118.

Hiei, Y., Ohta, S., Komari, T. and Kumashiro, T. 1994. Efficient transformation of rice (*Oryza sativa* L.) mediated by *Agrobacterium* and sequence analysis of the boundaries of the T-DNA. Plant J. 6: 271–282.

Jiang, J., Gill, B.S., Wang, G.L, Ronald, P.C. and Ward, D.C. 1995. Metaphase and interphase fluorescence in situ hybridization mapping of the rice genome with bacterial artificial chromosomes. Proc. Natl. Acad. Sci. USA 92: 4487–4491.

Kitajima, T., Miyazaki, Y., Yamamoto, M. and Watanabe, Y. 2003a. Rec8 cleavage by separase is required for meiotic nuclear divisions in fission yeast. EMBO J. 22: 5643–5653.

Kitajima, T.S., Yokobayashi, S., Yamamoto, M. and Watanabe, Y. 2003b. Distinct cohesin complexes organize meiotic chromosome domains. Science 300: 1152–1155.

Klein, F., Mahr, P., Galova, M., Buonomo, S.B.C., Michaelis, C., Nairz, K. and Nasmyth, K. 1999. A central role for cohesions in sister chromatid cohesion, formation of axial elements and recombination during yeast meiosis. Cell 98: 91–103.

Kohli, A., Twyman, R.M., Abranches, R., Wegel, E., Stoger, E. and Christou, P. 2003. Transgene integration, organization and interaction in plants. Plant Mol. Biol. 52: 247–258.

Laemmli, U.K. 1970. Cleavage of structural proteins during the assembly of the head of bacteriophase T4. Nature 227: 680–685.

Lavoie, B.D., Hogan, E. and Koshland, D. 2002. *In vivo* dissection of the chromosome condensation machinery: reversibility of condensation distinguishes contributions of condensin and cohesin. J. Cell. Biol. 156: 805–815.

Lee, J., Iwai, T., Yokota, T. and Yamashita, M. 2003. Temporally and spatially selective loss of Rec8 protein from meiotic chromosome during mammalian. J. Cell. Sci. 116: 2781–2790.

Lee, T.Y. and Orr-Weaver, T.L. 2001. The molecular basis of sister chromatid cohesion. Annu. Rev. Cell. Dev. Biol. 17: 753–777.

Li, W., Yang, X., Lin, Z., Timofejeva, L., Xiao, R., Makaroff, C., , A. and Ma, H. 2005. The *AtRAD51C* gene is required for normal meiotic chromosome synapsis and double-stranded break repair in Arabidopsis. Plant Physiol. 138: 965–976.

Ma, H. 2005. Molecular genetic analyses of microsporogenesis and microgametogenesis of flowering plants. Plant Biol. 56: 393–434.

Mckim, K.S., Green-Marroquin., B.L., Sekelsky, J.J., Chin, G., Steinberg, C., Khodosh, R. and Hawley, R.S. 1998. Meiotic synapsis in the absence of recombination. Science 279: 876–878.

Michaelis, C., Ciosk, R. and Nasmysh, K. 1997. Cohesions: chromosomal proteins that prevent premature separation of sister chromatids. Cell 91: 35–45.

Mito, Y., Sugimoto, A. and Yamamoto, M. 2003. Distinct developmental function of two *Caenorhabditis elegans* homologs of the cohesin subunit Scc1/Rad21. Mol. Biol. Cell 14: 2399–2409.

Murray, M.G. and Thompson, W.F. 1980. Rapid isolation of high molecular weight plant DNA. Nucl. Acids Res. 8: 4321–4325.

Nasmyth, K. 2001. Disseminating the genome: joining, resolving and separating sister chromatids during mitosis and meiosis. Annu. Rev. Genet. 35: 673–745.

Nasmyth, K. 2002. Segregating sister genomes: the molecular biology of chromosome separation. Science 297: 559–565.

Nonomura, K., Nakano, M., Fukuda, T., Eiguchi, M., Miyao, A., Hirochika, H. and Kurata, N. 2004. The novel gene *homologous pairing aberrantion in rice meiosis 1* of rice encodes a putative coiled-coil protein required for homologous pairing in meiosis. Plant Cell 16: 1008–1020.

Parisi, S., McKay, M.J., Molnar, M., Thompson, M.A., van der Spek, P.J., van Drunen-Schoenmaker, E., Kanaar, R., Lehmann, E., Hoeijmakers, J.H. and Kohli, J. 1999. Rec8p, a meiotic recombination and sister chromatid cohesion phosphoprotein of the Rad21p family conserved from fission yeast to humans. Mol. Cell. Biol. 19: 3515–3528.

Pasierbek, P., Jantsch, M., Melcher, M., Schleiffer, A., Schweizer, D. and Loidl, J. 2001. A *Caenorhabditis elegans* cohesion protein with functions in meiotic chromosome pairing and disjunction. Genes Dev. 15: 1349—1360.

Pawlowski, W.P., Golubovskaya, I.N., Timofejeva, L., Meeley, R.B., Sheridan, W.F. and Cande, W.Z. 2004. Coordination of meiotic recombination, pairing and synapsis by PHS1. Science 2004: 89–92.

Petronczki, M., Siomos, M. and Nasmyth, K. 2003. The molecular biology of chromosome segregation in meiosis. Cell 112: 423–440.

Prieto, I., Suja, J.A., Pezzi, N., Kremer, L., Martinez, A.C., Rufas, J.S. and Barbero, J.L. 2001. Mammalian STAG3 is a cohesin specific to sister chromatid arms in meiosis I. Nat. Cell. Biol. 3: 761–766.

Revenkova, E., Eijpe, M., Heyting, C., Gross, B. and Jessberger, R. 2001. Novel meiosis-specific isoform of mammalian SMC1. Mol. Cell. Biol. 21: 6984–6998.

Ross, K.J., Fransz, P. and Jones, G.H. 1996. A light microscopic atlas of meiosis in *Arabidopsis thaliana*. Chr. Res. 4: 551–559.

Salekdeh, G.H., Sinopongco, J., Wade, L.J., Ghareyazie, B. and Bennett, J. 2002. Proteomic analysis of rice leaves during drought stress and recovery. Proteomics 2: 1131–1145.

Shishido, R., Sano, Y. and Fukui, K. 2000. Ribosomal DNAs: an exception to the conservation of gene order in rice genomes. Mol. Gen. Genet. 263: 586–591.

Takaiwa, F., Oono, K., Lida, Y. and Sugiura, M. 1985. The complete nucleotide sequence of a rice 25S rRNA gene. Gene 37: 55–259.

Tanaka, T., Maria, C.P., Wirth, K. and Nasmyth, K. 1999. Identification of cohesin association sites at centromeres and along chromosome arms. Cell 98: 847–858.

Tomonaga, T., Nagao, K., Kawasaki, Y., Furuya, K., Murakami, A., Morishita, J., Yuasa, T., Sutani, T., Kearsey, S.E., Uhlmann, F., Nasmyth, K. and Yanagida, M. 2000. Characterzation of fission yeast cohesion: essential anaphase proteolysis of Rad21 phosphorylated in the S phase. Genes Dev. 14: 2757–2770.

Uhlmann, F. 2001. Chromosome cohesion and segregation in mitosis and meiosis. Curr. Opin. Cell. Biol. 13: 754–761.

Uhlmann, F. and Nasmyth, K. 1998. Cohesion between sister chromatids must be established during DNA replication. Curr. Biol. 8: 1095–1101.

Uhlmann, F., Wernic, D. and Poupart, M.A. 2000. Cleavage of cohesin by the CD clan protease separin triggers anaphase in yeast. Cell 103: 375–386.

Watanabe, Y. 2004. Modifying sister chromatid cohesion for meiosis. J. Cell Sci. 117: 4017–4023.

Watanabe, Y. and Nurse, P. 1999. Cohesin Rec8 is required for reductional chromosome segregation at meiosis. Nature 400: 461–464.

Watanabe, Y., Yokobayashi, S., Yamamoto, M. and Nurse, P. 2001. Pre-meiotic S phase is linked to reductional chromosome segregation and recombination. Nature 409: 359–363.

Wesley, S.V., Helliwell, C.A., Smith, N.A., Wang, M., Rouse, D.T., Liu, Q., Gooding, P.S., Singh, S.P., Abbott, D. and Stoutjesdijk, P.A. 2001. Construct design for efficient, effective and high-throughput gene silencing in plants. Plant J. 27: 581–590.

Worrall, D.M. 1996. Extraction of recombinant proteins from bacteria. In: S. Doonan (Ed.), Protein Purification Protocols, Humana, New Jersey, pp. 31–37.

Yang, Y., Li, R. and Qi, M. 2000. *In vivo* analysis of plant promoters and transcription factors by agroinfiltration of tobacco leaves. Plant J. 22: 543–551.

Yu, H. and Koshland, D.E. 2003. Meiotic condensin is required for proper chromosome compaction, SC assembly and resolution of recombination-dependent chromosome linkages. J. Cell. Biol. 163: 937–947.

Zhang, L.R., Tao, J.Y. and Wang, T. 2004. Molecular characterization of *OsRAD21–1*, a rice homologue of yeast *RAD21* essential for mitotic chromosome cohesion. J. Exp. Bot. 55: 1149–1152.

Zickler, D. and Kleckner, N. 1999. Meiotic chromosomes: integrating structure and function. Annu. Rev. Genet. 33: 603–754.